

Electronic Supplementary Information (ESI)

Photoresponsive Triazole-Based Donor–Acceptor Molecules: Color Change and Heat/Air-Stable Diradicals

Ning-Ning Zhang,^{a,d} Rong-Jian Sa,^{*c} Shan-Shan Sun,^b Ming-De Li,^{*b} Ming-Sheng Wang,^{*a} and Guo-Cong Guo^{*a}

a. State Key Laboratory of Structural Chemistry, Fujian Institute of Research on the Structure of Matter Chinese Academy of Sciences.

b. Department of Chemistry and Key Laboratory for Preparation and Application of Ordered Structural Materials of Guangdong Province, Shantou University.

c. Institute of Oceanography, Ocean college, Minjiang University.

d. University of Chinese Academy of Sciences.

Abstract: Photoinduced generation of stable radicals is important for photochromism, photoswitching and other applications, but was only limited to a few systems. An unprecedented series of triazole-based donor–acceptor organic molecules were found to form heat/air-stable triplet diradicals in the solid state and show clear color change through photoinduced intramolecular charge separation, which was confirmed by electron spin resonance studies, ultrafast laser flash photolysis analyses and density functional theoretical calculations. In these molecules, electron-withdrawing substituents were more beneficial to the photoinduced charge separation than electron-donating ones. Moreover, a high molecular dipole moment was more conducive to the photoinduced charge separation in the presence of an electron-withdrawing substituent.

Table of Contents

1. Experimental Procedures	S3
1.1 Materials.....	S3
1.2 Methods.....	S3
1.3 Synthesis.	S4
Scheme S1	S5
1.4 Graphs.	S6
Fig. S1	S6
Fig. S2.....	S6
Fig. S3.....	S7
Fig. S4.....	S7
Fig. S5.....	S7
Fig. S6.....	S8
Fig. S7.....	S8
Fig. S8.....	S8
Fig. S9.....	S9
Fig. S10.....	S9
Fig. S11.....	S10
Fig. S12.....	S10
Fig. S13.....	S10
Fig. S14.....	S11
Fig. S15.....	S11
Fig. S16.....	S12
Fig. S17.....	S12
Fig. S18.....	S13
Fig. S19.....	S13
Fig. S20.....	S14
Fig. S21.....	S14
Fig. S22.....	S15
Table S1	S16
Table S2.....	S16
Table S3.....	S17
Table S4.....	S18
Table S5.....	S19
Table S6.....	S20
Table S7.....	S21
Table S8.....	S22
2. References.....	S25

1. Experimental Procedures

1.1 Materials.

Azide compounds were prepared according to the previously reported procedure.¹ Water was used after deionization and distillation. All other chemicals were purchased commercially and used without further treatment.

Caution! Azide compounds, which are potentially hazardous, should be carefully used. They should be handled with a plastic spoon.

1.2 Methods.

IR data were obtained by a PerkinElmer Spectrum One FT-IR spectrophotometer over the range of 4000–400 cm^{-1} with pure KBr pellets as the baseline. ^1H NMR and ^{13}C NMR spectra were measured by an Avance III NMR spectrometer operating at 400 MHz. Mass spectra were recorded with a DECAX-30000 LCQ Deca XP ion trap mass spectrometer. TG analyses were performed on a NETZSCH STA 449C simultaneous thermal analyzer with Al_2O_3 crucibles under N_2 (20 $\text{mL}\cdot\text{min}^{-1}$) at a heating rate of 10 $\text{K}\cdot\text{min}^{-1}$. PXRD patterns were collected at room temperature on a Rigaku MiniFlex II diffractometer using $\text{Cu } K\alpha$ radiation ($\lambda = 1.5406 \text{ \AA}$). Simulated PXRD patterns were derived from the Mercury Version 3.5.1 software using the X-ray single crystal diffraction data. Electronic absorption spectra were measured in the diffuse reflectance mode at room temperature on a Perkin-Elmer Lambda 900 UV/vis/NIR spectrophotometer with an integrating sphere attachment and BaSO_4 as a reference. ESR spectra were recorded on a Bruker ER-420 spectrometer with a 100 kHz magnetic field in the X band. A PLSSXE300C 300 W Xe lamp system equipped with an IR filter ($\sim 102 \text{ mW cm}^{-2}$) was used to illuminate samples to record various spectra. Solid-state Raman spectra were measured on a Labram HR800 Evolution UV/vis/NIR microcofocal Raman spectrometer by a 785 nm laser source at room temperature.

The fs-TA spectra were measured using a femtosecond regenerative amplified Ti: sapphire laser system in which the amplifier was seeded with 80 fs laser pulses from an oscillator laser system. The laser probe pulse was produced by utilizing $\sim 12.5\%$ of the amplified 800 nm laser pulses to generate a white-light continuum (320–680 nm) by a CaF_2 crystal. Then, this probe beam was split into two parts before traversing the sample. One probe beam passed through the sample, while the other probe laser beam passed through the reference spectrometer to monitor the fluctuations of the probe beam intensity. For the experiments in this study, a singlet crystal sample was fixed on a quartz plate. The sample was excited by a 310 nm pump beam, and the power was approximately 1 mW. To obtain the time constant of the different intermediates, a sum of convoluted exponentials function was used to fit a kinetic trace at the selected wavelength as follows (eq1):

$$S(t) = e^{-\left(\frac{t-t_0}{t_p}\right)^2} \times \sum_i A_i e^{-t-t_0/t_i}$$

where t_p is the instrument response time; t_0 is time zero; and A_i and t_i are amplitudes and decay times, respectively. The fitting curve is given in Fig. 3f.

X-ray crystallographic study. The intensity data sets were collected on an Agilent Technologies SuperNova Dual Wavelength CCD diffractometer with graphite-monochromated $\text{Cu } K\alpha$ radiation ($\lambda = 1.54178 \text{ \AA}$) using the $\omega-2\theta$ scan technique and reduced by the CrysAlisPro software.² The data set was corrected for Lorentz and polarization factors and for the absorption by the numerical method. The structures were solved by the direct method and refined by the full-matrix least squares on F^2 using the Siemens SHELXTLTM Version 5 package of crystallographic software³ using anisotropic thermal parameters for all non-hydrogen atoms. Hydrogen atoms were added geometrically and refined using the riding model. The program PLATON⁴ was used to check the structures for possible missing symmetry, and no such structure was found.

The entry of CCDC-1570942, 1857195 contains the supplementary crystallographic data for **1**. These data can be obtained free of charge from <http://www.ccdc.cam.ac.uk/conts/retrieving.html> or from the Cambridge Crystallographic Data Centre, 12, Union Road, Cambridge CB2 1EZ, U.K. Fax: (Internet) +44-1223/336-033. E-mail: deposit@ccdc.cam.ac.uk.

Theoretical computations. Oscillator strengths (f), ESP, spin density, and reduced density gradient were calculated using the Gaussian 09 software suite.⁵ Oscillator strengths (f) of the monomer of crystal **1** were achieved by time-dependent density functional theoretical (TD-DFT) calculations at the M062X/defTZVP level without structural optimization and processed with the GaussView 5.0 software. The ESP and spin density were calculated at the CAM-B3LYP/6-31G(d,p) level using the geometry optimized at the M062X/6-311G(d,p) level (vibrational analysis was performed to confirm each optimized stationary point to be a minimum). To obtain plots of the electron density (ρ) and reduced density gradient [$s = 1/(2(3\pi^2)^{1/3})|\nabla\rho|/\rho^{4/3}$],⁶ DFT calculations at the B3LYP/6-31G(d,p) level were performed for a selected set of **1**, and the results were analyzed by Multiwfn.⁷ The calculation of Mayer bond orders of monomer **1** was carried out at M06-2X/def2TZVP level. The analysis of Mayer bond orders and bond lengths was via Multiwfn and GaussView 5.0, respectively.

The DOS and linear optical properties were calculated using the CASTEP package.⁸ The structural model for **1** was built directly from the single-crystal X-ray diffraction data. The exchange-correlation energy was described by the PBE functional within the GGA.^{9,10} The norm conserving pseudopotentials were chosen to modulate the electron-ion interaction.^{11,12} The orbital electrons of C $2s^22p^2$, H $1s^1$, and N $2s^22p^3$ were treated as valence electrons. The plane-wave cutoff energy was 700 eV, and the threshold of 5×10^{-7} eV was set for the self-consistent field convergence of the total electronic energy. The numerical integration of the Brillouin zone was performed using $3 \times 2 \times 1$ Monkhorst-Pack k -point meshes for **1**. The Fermi level was selected as the reference and set to 0 eV by default.

Linear optical properties were described in terms of the complex dielectric function $\varepsilon = \varepsilon^{\text{Re}} + i\varepsilon^{\text{Im}}$. The imaginary part of the dielectric function $\varepsilon^{\text{Im}}(\omega)$ was given by the following equation (eq2):

$$\varepsilon^{\text{Im}}(\omega) = 4 \left(\frac{\pi e}{m\omega} \right)^2 \sum_{v,c} \int_{BZ} 2dk / (2\pi)^3 |e \cdot M_{cv}(k)|^2 \delta(E_c(k') - E_v(k) - \hbar\omega),$$

where \int is the sum over the valence bands (v) and conduction bands (c), ω is the optical frequency, m is the electron mass, \int is the integration over the k vectors in Brillouin zone (BZ), $e \cdot M_{cv}(k)$ is the electron transition moment between v and c at k point, and the δ function is the energy difference between the v and c at the k point with the absorption of a quantum $\hbar\omega$.

The Kramers-Kronig transform was used to obtain the real part $\varepsilon^{\text{Re}}(\omega)$ of the dielectric function as follows (eq3):

$$\varepsilon^{\text{Re}}(\omega) = 1 + \frac{2}{\pi} p \int_0^\infty \frac{\omega' \varepsilon^{\text{Im}}(\omega')}{\omega'^2 - \omega^2} d\omega',$$

where p in front of the integral means the principal value. The absorbance $\alpha(\omega)$ was given in the following equation (eq4):¹³

$$\alpha(\omega) = \frac{\varepsilon^{\text{Im}}(\omega)\omega}{n(\omega)C},$$

where C and $n(\omega)$ are the velocity of light and refractive index, respectively. The $n(\omega)$ was expressed as follows (eq5):

$$n(\omega) = \frac{1}{\sqrt{2}} \left[(\varepsilon^{\text{Re}}(\omega)^2 + \varepsilon^{\text{Im}}(\omega)^2)^{1/2} + \varepsilon^{\text{Re}}(\omega) \right]^{1/2}.$$

The smearing width was set to 0.2 eV for Figure 4a and 0.05 eV for Figure 4b. Other parameters were set to default values.

1.3 Synthesis.

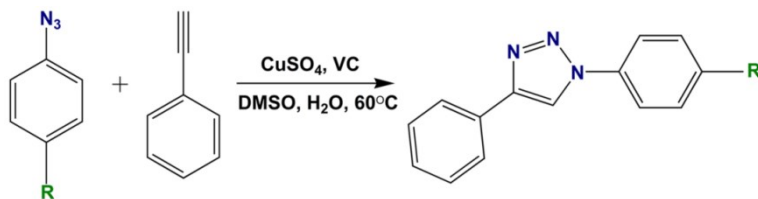
1-(4-cyanophenyl)-4-phenyl-1,2,3-triazole (1). Compound **1** was prepared by a 1,3-dipolar cycloaddition reaction reported by Sharpless et al.³³ Typically, 4-cyanophenyl azide (0.720 g, 5 mmol) and phenylacetylene (0.510 g, 5 mmol) were dissolved in 25 mL of a 4:1 DMSO/water mixture. Whereafter, sodium ascorbate (0.099 g, 0.5 mmol, in 0.5 mL of water) and CuSO_4 (0.010 g, 0.06 mmol, in 0.3 mL of water) were added to the solution in turn. The obtained solution was stirred at 333 K for 1 d and then poured into 100 mL of ice-cold water. Yellow precipitate of **1** was isolated by filtering the solution and then washed with vast cold water and dried in air. Yield: 80% (based on

4-cyanophenyl azide). IR (KBr, cm^{-1}): 3125 m, 3096 w, 2227 s, 1608 s, 1516 s, 1483 m, 1449 w, 1430 w, 1406 m, 1348 w, 1319 m, 1295 w, 1271 w, 1228 s, 1179 m, 1112 w, 1087 w, 1070 w, 1037 s, 987 m, 969 w, 919 w, 836 s, 776 s, 692 s, 549 s, 519 w. $^1\text{H-NMR}$ (d^6 -DMSO) δ/ppm (Figure S1): 9.47 (s, 1H, triazole-H), 8.18 (m, 3H, Ph-H), 7.96 (m, 2H, Ph-H), 7.47 (dt, 3H, Ph-H). ESI-MS (DMSO): 247.098 $[\text{M}+\text{H}]^+$. Crystals suitable for single-crystal X-ray diffraction analysis were grown by slowly volatilizing its CH_3CN solution at room temperature.

1-(4-amidophenyl)-4-phenyl-1,2,3-triazole (2). Bright yellow green powder of **2** was prepared using a method similar to that of **1**, just replacing 4-cyanophenyl azide (0.720 g, 5 mmol) with 4-amidophenyl azide (0.810 g, 5 mmol). Yield: 85% (based on 4-amidophenyl azide). IR (KBr, cm^{-1}): 3460 s, 3183 w, 3127 w, 1663 s, 1615 s, 1523 m, 1481 w, 1400 s, 1229 s, 1179 w, 1038 m, 998 w, 917 w, 857 s, 825 m, 765 s, 694 s, 664 w, 533 m. $^1\text{H-NMR}$ (d^6 -DMSO) δ/ppm (Figure S1): 9.47 (s, 1H, triazole-H), 8.12 (m, 4H, Ph-H), 7.97 (m, 2H, NH_2 -H), 7.53 (t, 2H, Ph-H), 7.42 (t, 1H, Ph-H). ESI-MS (DMSO): 263.094 $[\text{M}+\text{H}]^+$. Crystals suitable for single-crystal X-ray diffraction analysis were not obtained.

1-(4-carboxyphenyl)-4-phenyl-1,2,3-triazole (3). Yellowish green powder of **3** was prepared using a method similar to that of **1**, just replacing 4-cyanophenyl azide (0.720 g, 5 mmol) with 4-carboxyphenyl azide (0.815 g, 5 mmol). Yield: 90% (based on 4-carboxyphenyl azide). IR (KBr, cm^{-1}): 3139 m, 3081 w, 2832 w, 2680 w, 2548 w, 1700 s, 1608 s, 1523 w, 1439 m, 1320 m, 1295 s, 1234 s, 1178 w, 1117 w, 1042 m, 990 m, 939 w, 862 m, 770 s, 685 m, 554 w, 502 w. $^1\text{H-NMR}$ (d^6 -DMSO) δ/ppm (Figure S1): 13.29 (s, 1H, COOH), 9.45 (s, 1H, triazole-H), 8.19 (d, 2H, Ph-H), 8.12 (d, 2H, Ph-H), 7.97 (d, 2H, Ph-H), 7.52 (t, 2H, Ph-H), 7.41 (t, 1H, Ph-H). ESI-MS (DMSO): 264.078 $[\text{M}-\text{H}]^-$. Crystals suitable for single-crystal X-ray diffraction analysis were not obtained.

1-(4-methoxyphenyl)-4-phenyl-1,2,3-triazole (4). Brown precipitate powder of **4** was prepared using a method similar to that of **1**, just replacing 4-cyanophenyl azide (0.720 g, 5 mmol) with 4-methoxyphenyl azide (0.745 g, 5 mmol). Yield: 20% (based on 4-methoxyphenyl azide). IR (KBr, cm^{-1}): 3122 m, 2958 w, 2832 w, 1608 w, 1525 s, 1482 w, 1298 m, 1235 s, 1185 m, 1109 w, 1034 s, 996 m, 920 w, 832 s, 769 s, 694 s, 618 w, 543 m. $^1\text{H-NMR}$ (d^6 -DMSO) δ/ppm (Figure S1): 9.21 (s, 1H, triazole-H), 7.95 (m, 2H, Ph-H), 7.87 (d, 2H, Ph-H), 7.50 (t, 2H, Ph-H), 7.38 (m, 1H, Ph-H), 7.18 (m, 2H, Ph-H), 3.82 (m, 3H, CH_3 -H). ESI-MS (DMSO): 252.113 $[\text{M}+\text{H}]^+$. Single crystals of **4** were grown by slowly volatilizing the filtrate at room temperature.



Scheme S1. Preparation of compounds **1–4**: VC = sodium ascorbate; R = $-\text{CN}$ (**1**) / $-\text{COONH}_2$ (**2**) / $-\text{COOH}$ (**3**) / $-\text{OCH}_3$ (**4**).

1.4 Graphs.

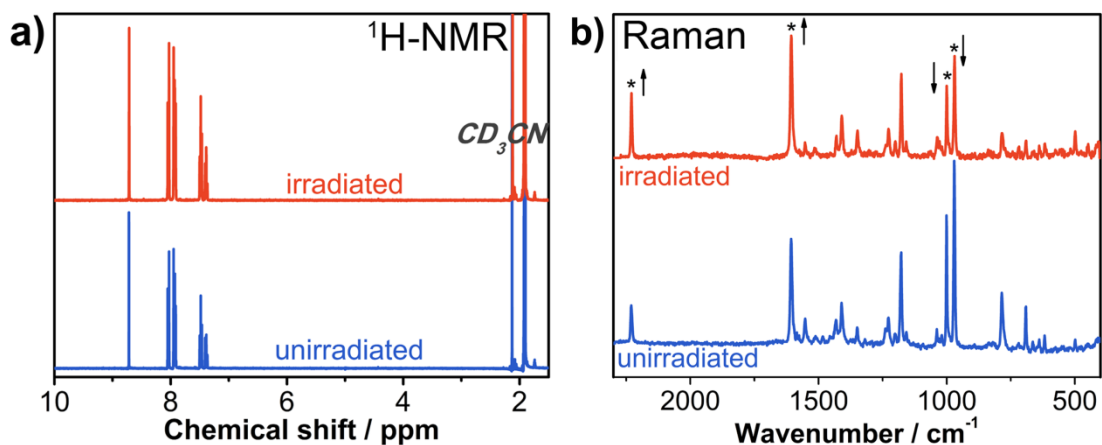


Fig. S1. For 1: a) $^1\text{H-NMR}$ spectra for $\text{CD}_3\text{CN-}d_3$ solution of unirradiated and irradiated powder samples. b) Raman spectra in the solid state before and after irradiation. All irradiation experiments were conducted under ambient conditions.

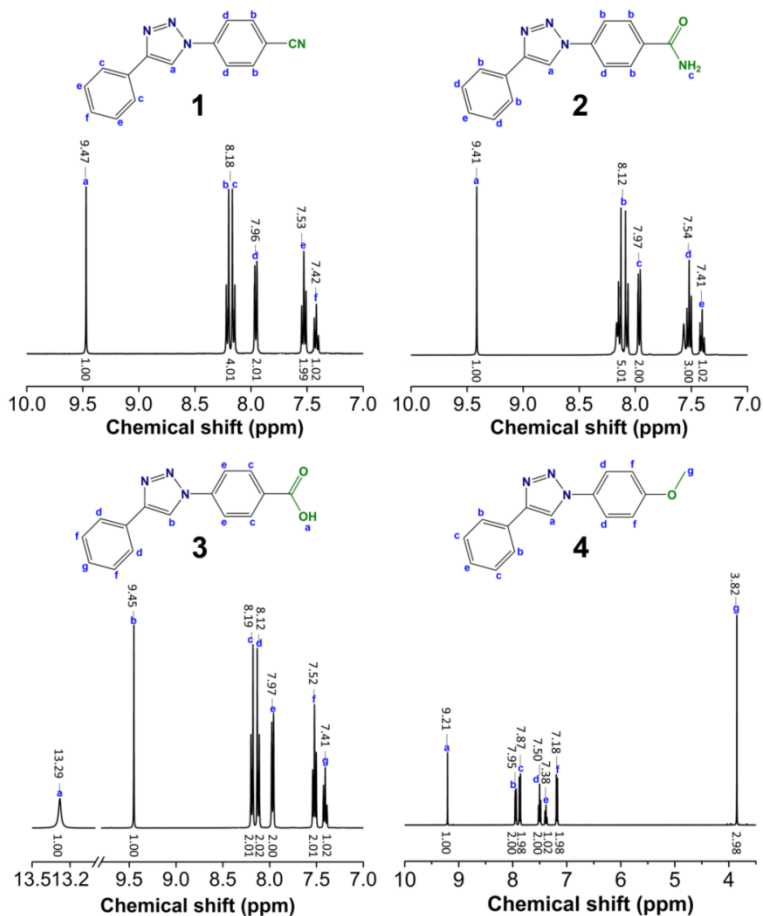


Fig. S2. $^1\text{H-NMR}$ spectra of the as-synthesized samples of 1–4 in d_6 -DMSO.

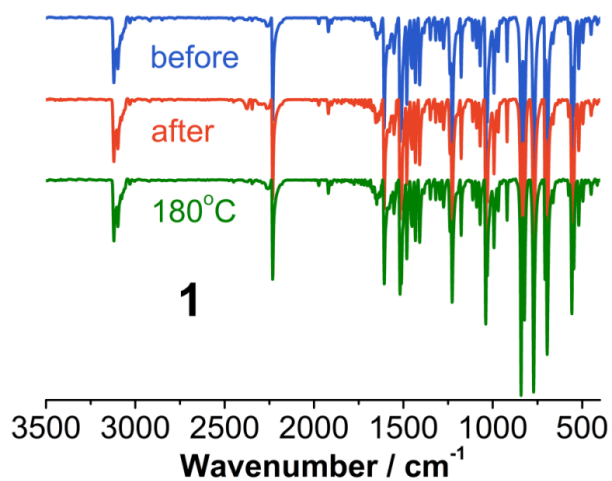


Fig. S3. IR spectra of **1** in the KBr matrix: before irradiation, after irradiation, and thermal annealing at 180 °C in air for 2 h after irradiation.

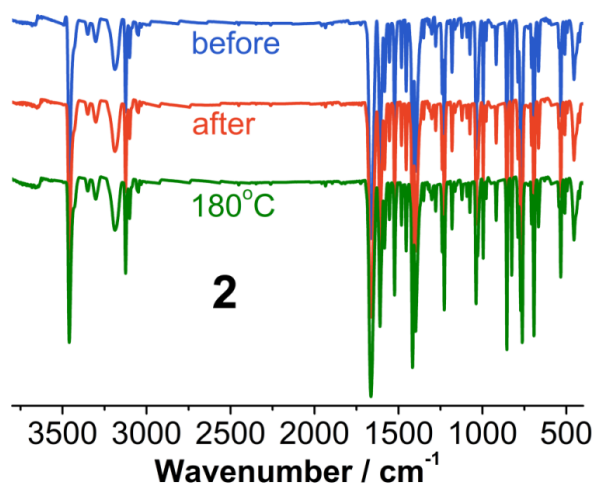


Fig. S4. IR spectra of **2** in the KBr matrix: before irradiation, after irradiation, and thermal annealing at 180 °C in air for 2 h after irradiation.

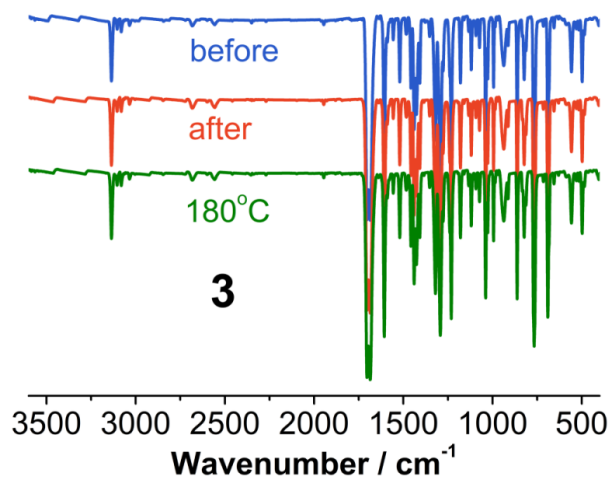


Fig. S5. IR spectra of **3** in the KBr matrix: before irradiation, after irradiation, and thermal annealing at 180 °C in air for 2 h after irradiation.

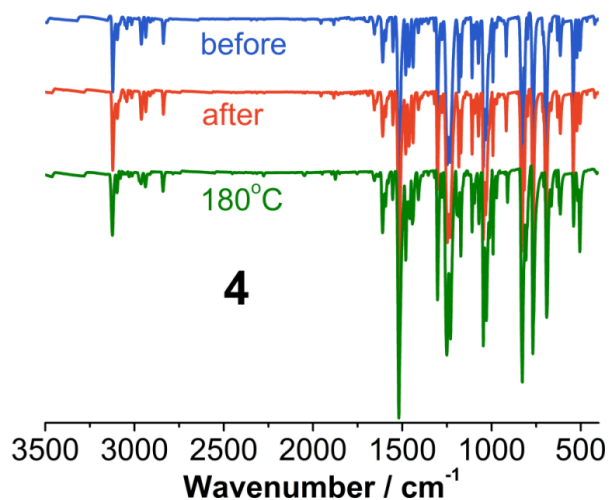


Fig. S6. IR spectra of **4** in the KBr matrix: before irradiation, after irradiation, and thermal annealing at 180 °C in air for 2 h after irradiation.

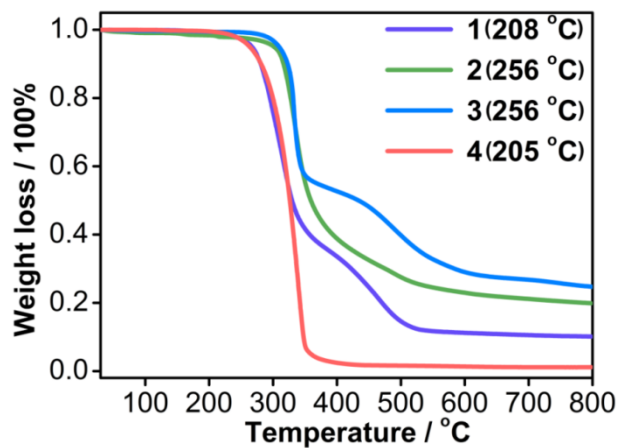


Fig. S7. Thermogravimetric curves of **1-4** under N₂ with heating rate of 10 °C/min. The highest stable temperatures were shown in brackets.

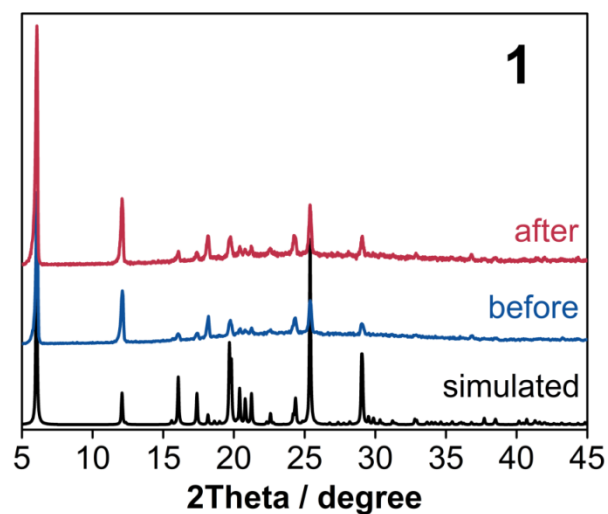


Fig. S8. PXRD spectra of the same sample of **1** before and after irradiation. The simulated pattern was derived from the single crystal X-ray diffraction data.

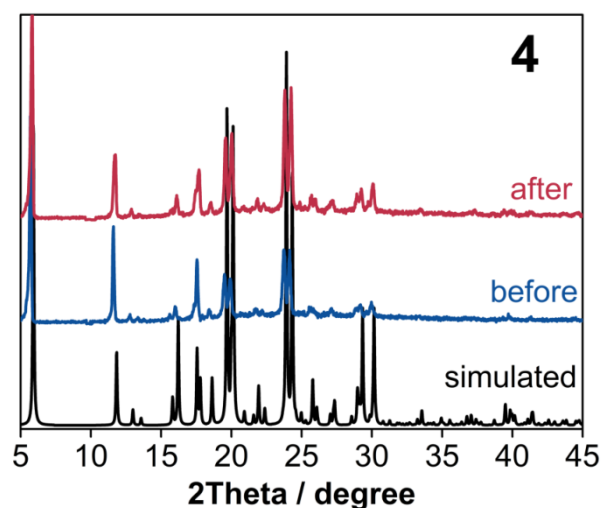


Fig. S9. PXRD spectra of the same sample of 4 before and after irradiation. The simulated pattern was derived from the single crystal X-ray diffraction data.

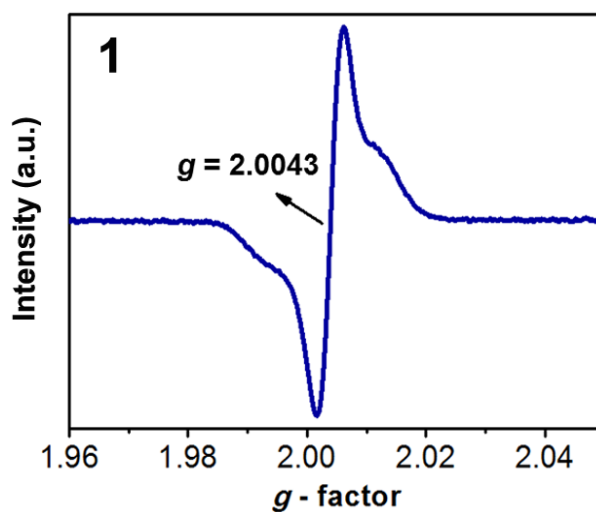


Fig. S10. ESR signal of 1 after the following treatment: the as-synthesized sample was thermally annealed at 120 °C in vacuum for 2 h and then irradiated by the Xe lamp for 30 min after cooling to the ambient temperature.

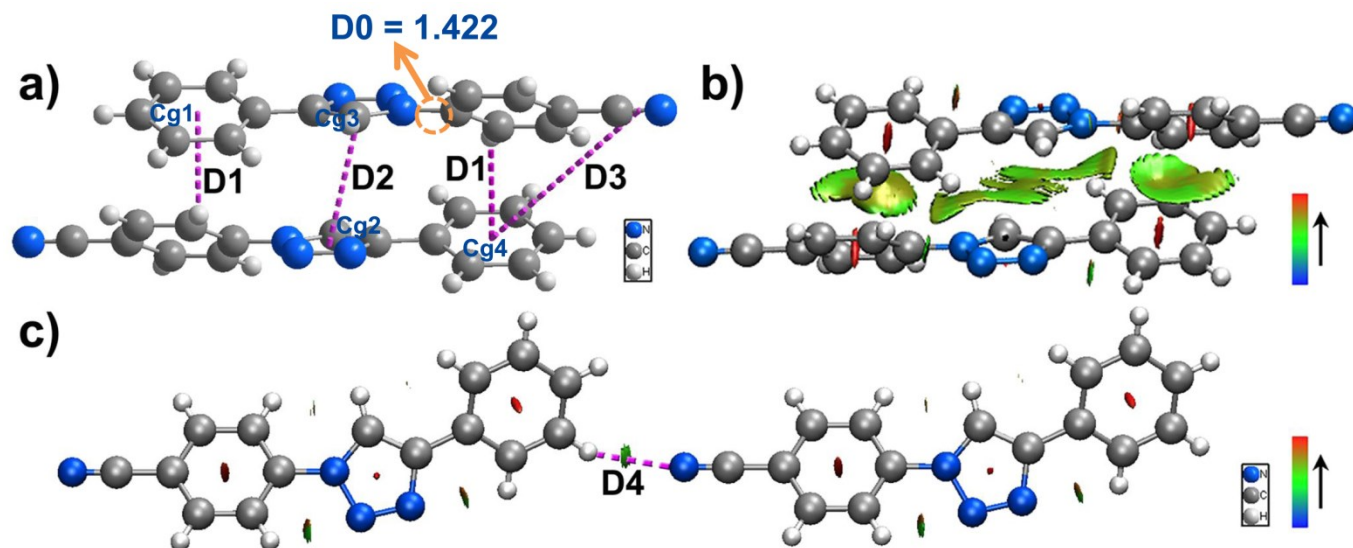


Fig. S11. For **1**: (a, c) The selected dimers from the crystal structure. The distances ($D1 = 2.76(1)$, $D2 = 3.76(2)$, $D3 = 6.61(4)$ and $D4 = 2.800$ Å) were marked by purple dash lines (Cg: the central point of rings). (b, c) Gradient isosurfaces ($s = 0.5$ a.u.) for dimers of **1**. The surfaces are colored on a blue-green-red (BGR) scale according to values of $\text{sign}(\lambda_2)\rho$, ranging from -0.04 to 0.02 a.u.. Blue indicates strong attractive interactions, and red indicates strong nonbonded overlap.

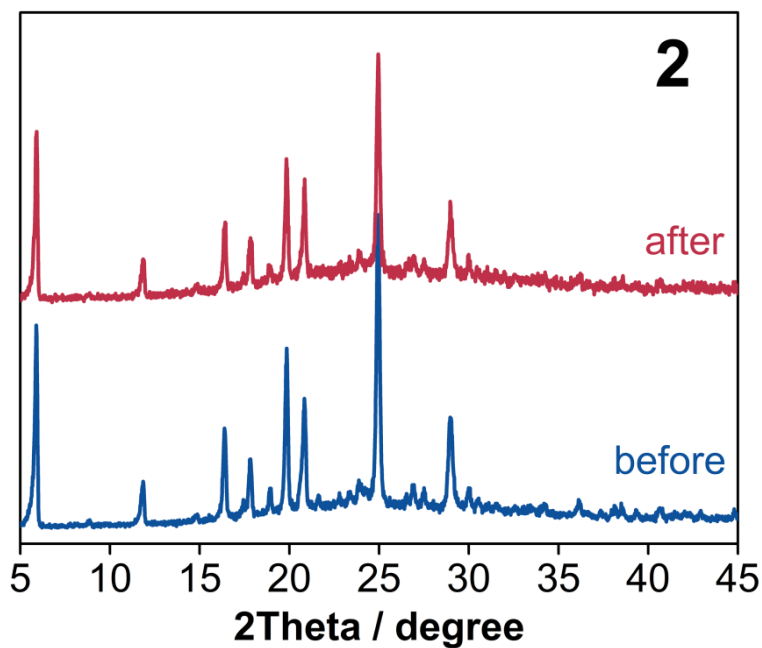


Fig. S12. PXRD patterns of the same sample of **2** before and after irradiation under ambient conditions.

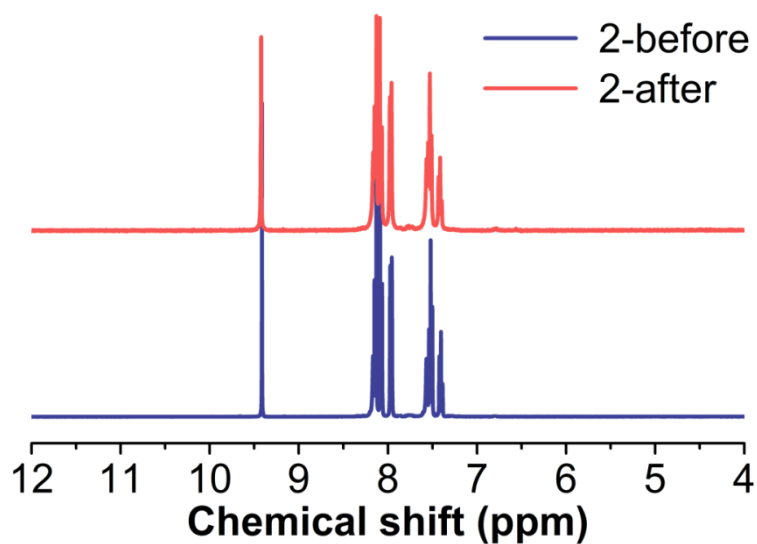


Fig. S13. ¹H-NMR spectra of **2** in DMSO-d₆ before and after irradiation under ambient conditions. Note: the sample was irradiated and then dissolved in DMSO-d₆.

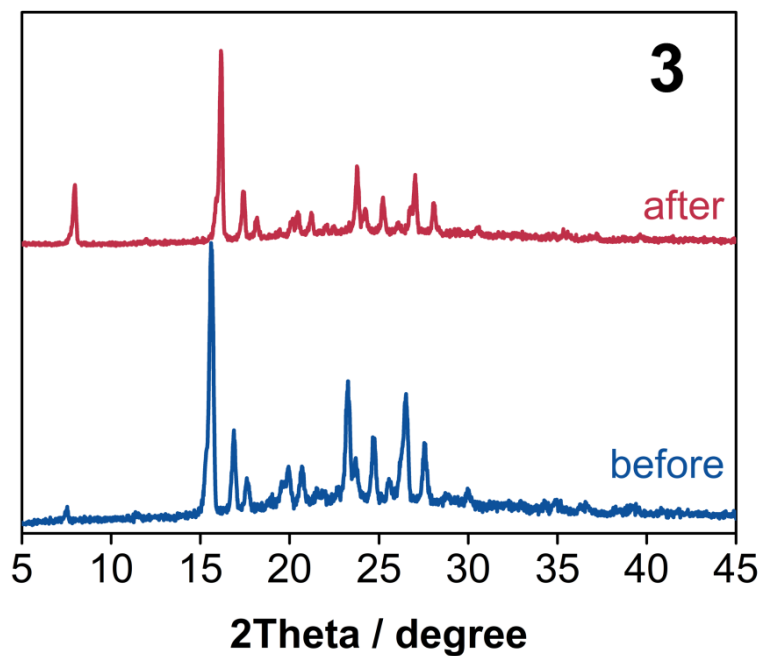


Fig. S14. PXRD patterns of the same sample of **3** before and after irradiation under ambient conditions.

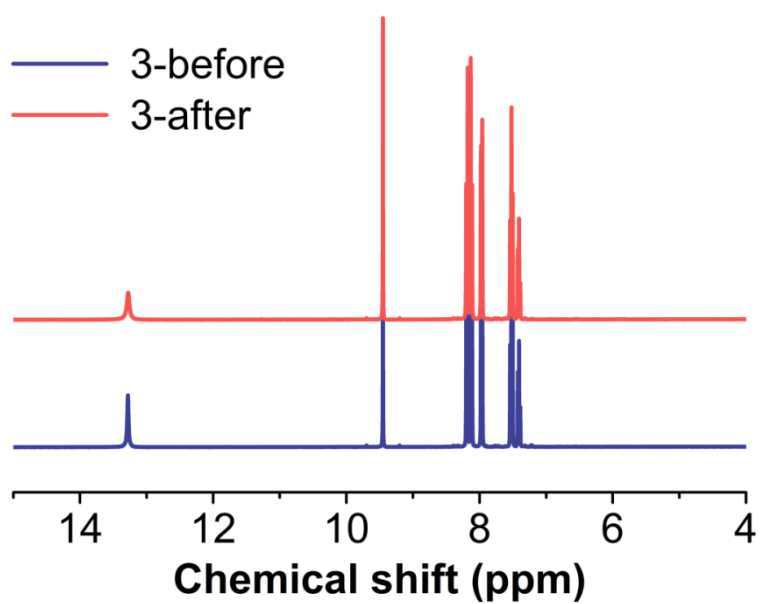


Fig. S15. ¹H-NMR spectra of **3** in DMSO-d₆ before and after irradiation under ambient conditions. Note: the sample was irradiated and then dissolved in DMSO-d₆.

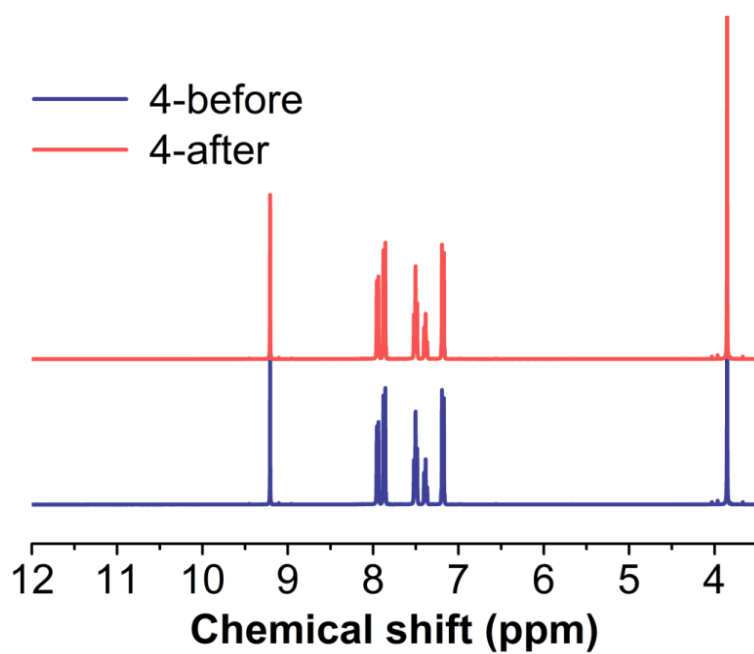


Fig. S16. $^1\text{H-NMR}$ spectra of **4** in DMSO-d_6 before and after irradiation under ambient conditions. Note: the sample was irradiated and then dissolved in DMSO-d_6 .

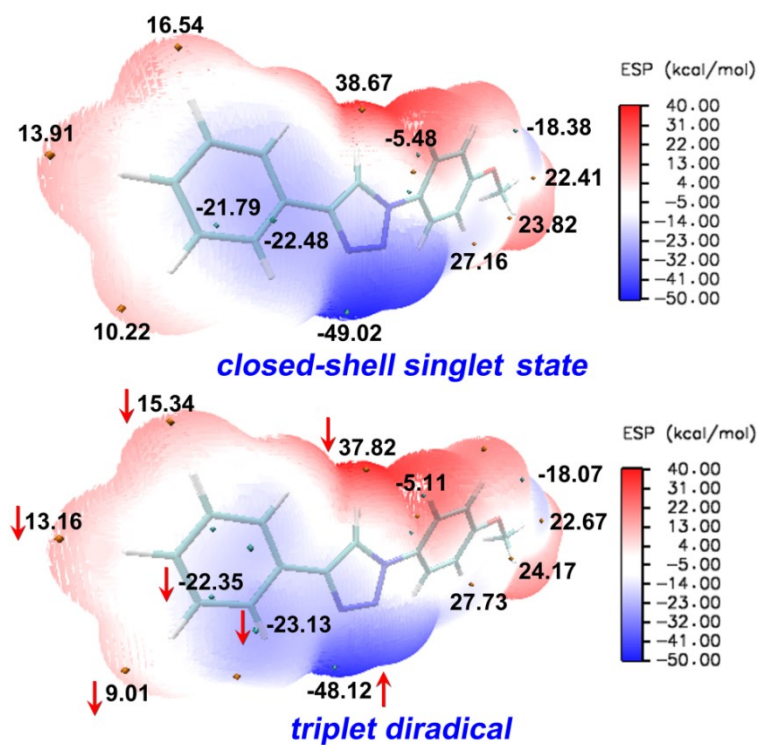


Fig. S17. Electrostatic potential surfaces of **4**. Significant surface local minima and maxima of ESP are represented as orange and cyan spheres, respectively.

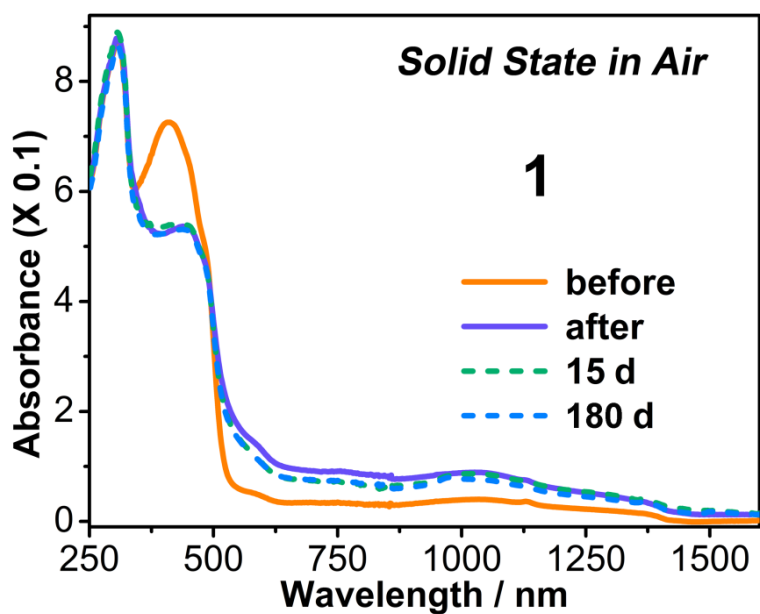


Fig. S18. Electronic absorption spectra of **1** in the solid state before and after irradiation under ambient conditions. The data for the irradiated samples after placing in dark in air for 15 and 180 d are also shown.

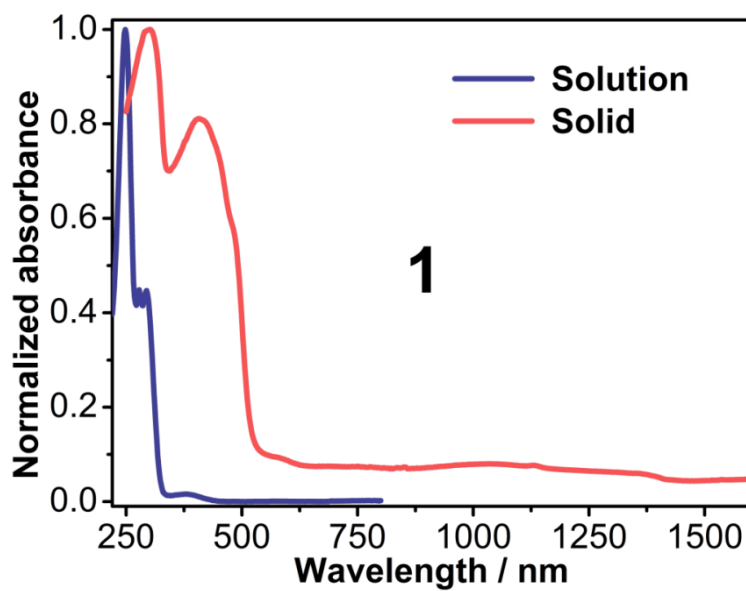


Fig. S19. Comparison of electronic absorption spectra of **1** in CH₃CN and the solid state.

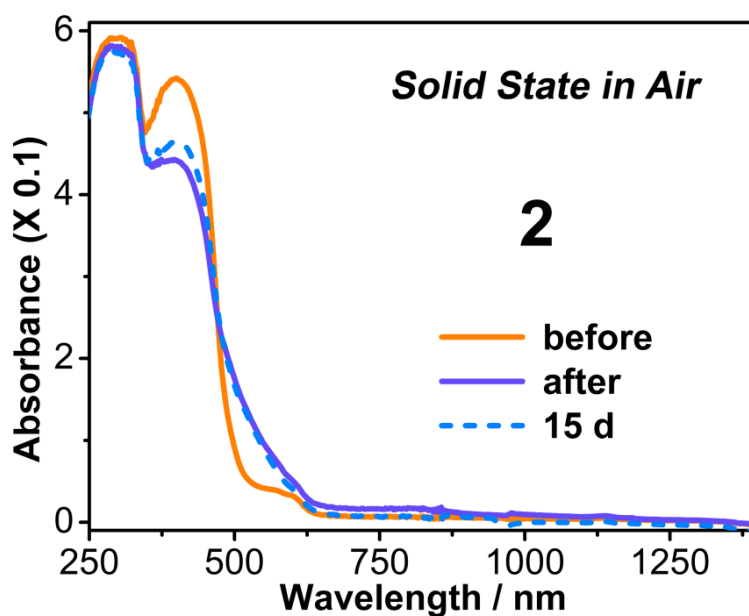


Fig. S20. Electronic absorption spectra of **2** in the solid state before and after irradiation under ambient conditions. The data for the irradiated samples after placing in dark in air for 15 d are also shown.

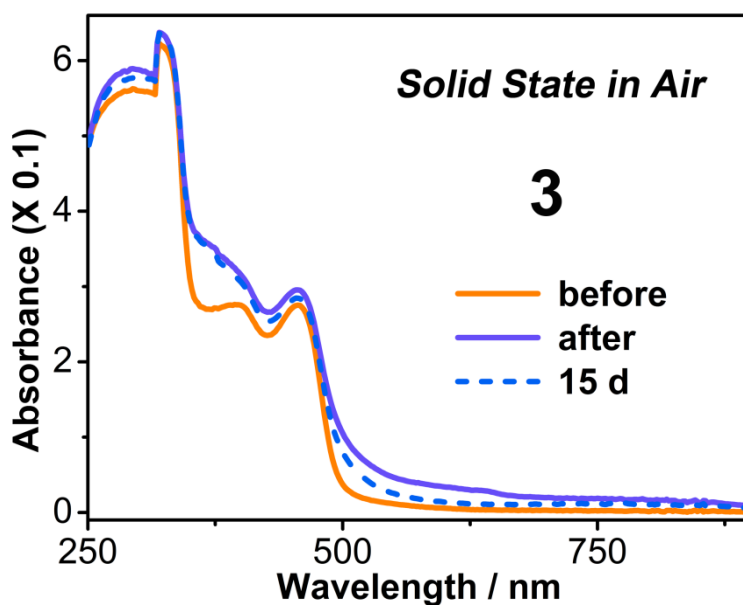


Fig. S21. Electronic absorption spectra of **3** in the solid state before and after irradiation under ambient conditions. The data for the irradiated samples after placing in dark in air for 15 d are also shown.

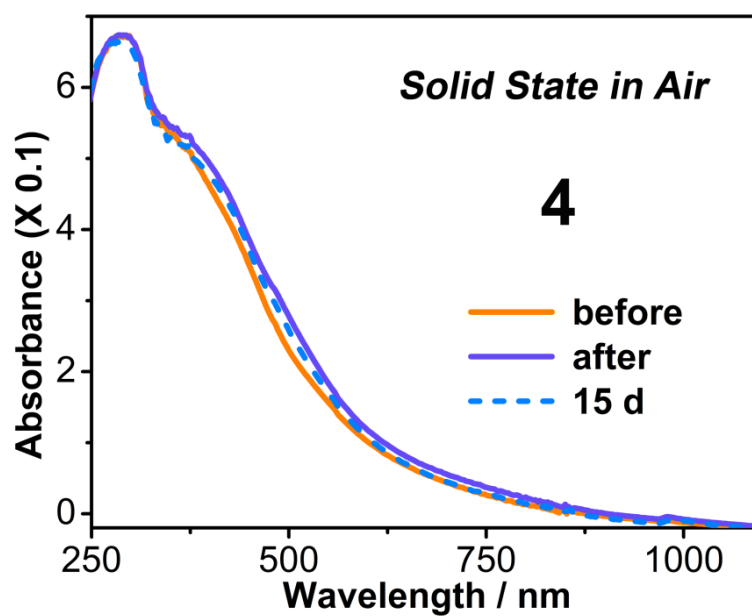


Fig. S22. Electronic absorption spectra of **4** in the solid state before and after irradiation under ambient conditions. The data for the irradiated samples after placing in dark in air for 15 d are also shown.

Table S1. Crystal data and structural refinements for 1.

Formula	C ₁₅ H ₁₀ N ₄
Mr	246.27
Crystal size (mm³)	0.42 × 0.29 × 0.11
Crystal system	Triclinic
Space group	P $\bar{1}$
a (Å)	5.7160(19)
b (Å)	7.308(3)
c (Å)	15.041(6)
α (deg)	101.473(9)
β (deg)	96.492(8)
γ (deg)	90.187(6)
V (Å³)	611.6(4)
D_{calcd} (g/cm³)	1.343
Z	2
F(000)	256
Abs coeff (mm⁻¹)	0.672
R₁^a	0.0367
ωR₂^b	0.1106
GOF on F²	0.992

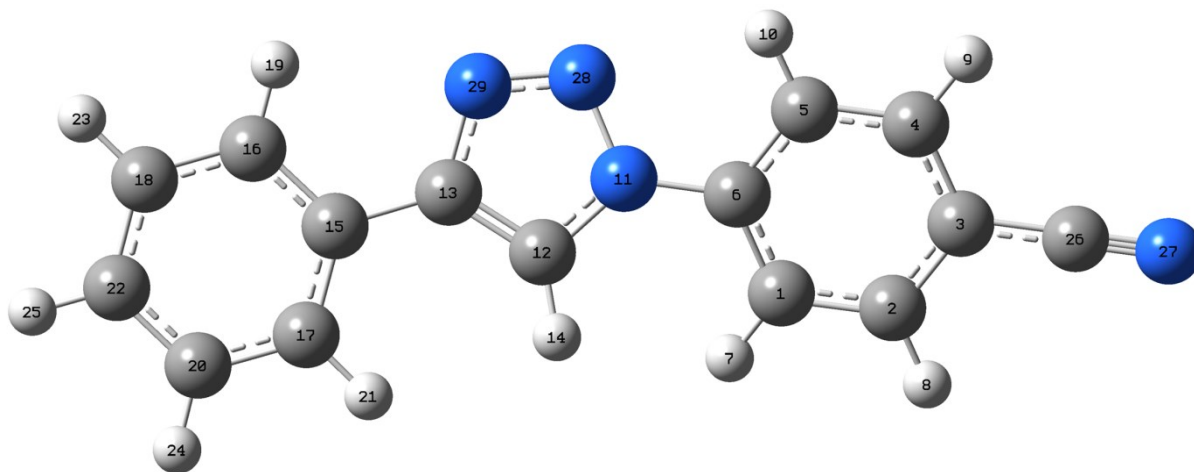
$$^a R_1 = \sum ||F_o| - |F_c|| / \sum |F_o|; \quad ^b \omega R_2 = \{ \sum \omega [(F_o)^2 - (F_c)^2]^2 / \sum \omega [(F_o)_2]^2 \}^{1/2}.$$

Table S2. Crystal data and structural refinements for 4.

Formula	C ₁₅ H ₁₃ N ₃ O
Mr	251.28
Crystal size (mm³)	0.20 × 0.18 × 0.10
Crystal system	Triclinic
Space group	P $\bar{1}$
a (Å)	5.6371(5)
b (Å)	7.4472(6)
c (Å)	15.0753(10)
α (deg)	93.055(6)
β (deg)	96.810(6)
γ (deg)	90.542(7)
V (Å³)	627.43(9)
D_{calcd} (g/cm³)	1.330
Z	2
F(000)	264
Abs coeff (mm⁻¹)	0.087
R₁^a	0.0482
ωR₂^b	0.1306
GOF on F²	1.076

$$^a R_1 = \sum ||F_o| - |F_c|| / \sum |F_o|; \quad ^b \omega R_2 = \{ \sum \omega [(F_o)^2 - (F_c)^2]^2 / \sum \omega [(F_o)_2]^2 \}^{1/2}.$$

Table S3. Mulliken charges of **1** in ground state and Mulliken charges and spin densities of **1** in the triplet diradical state.

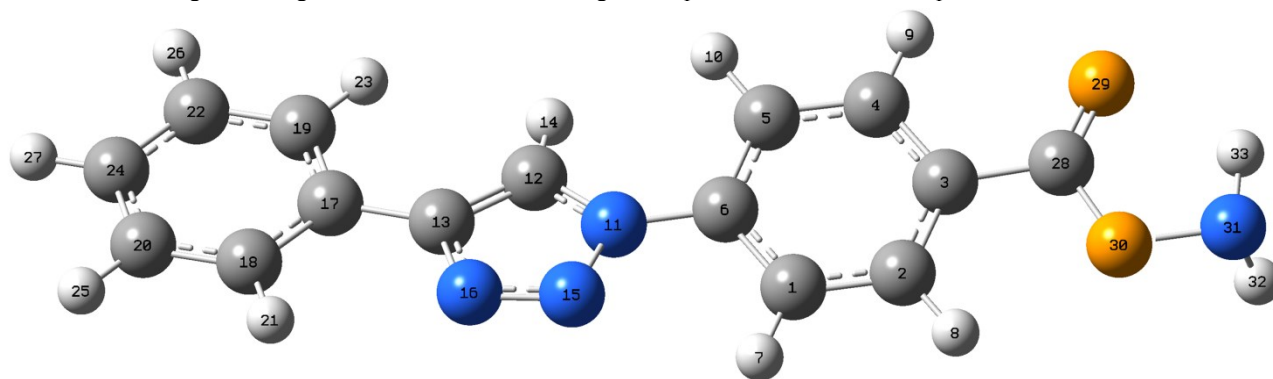


No.	Elements	Ground state	Triplet diradical	
		Mulliken charges	Mulliken charges	Spin population
1	C	-0.174873	-0.200040	0.121939
2	C	-0.151064	-0.162516	-0.067560
3	C	0.112103	0.082744	0.183013
4	C	-0.149602	-0.162002	-0.063691
5	C	-0.160976	-0.188032	0.119112
6	C	0.348426	0.327132	0.022731
7	H	0.195251	0.171190	-0.005779
8	H	0.196142	0.175208	0.002344
9	H	0.194863	0.173638	0.002127
10	H	0.200203	0.177625	-0.006226
11	N	-0.389637	-0.403986	0.060892
12	C	0.007815	0.011511	0.597874
13	C	0.170967	0.231603	0.284199
14	H	0.234088	0.233673	-0.027446
15	C	0.115356	0.110339	-0.041066
16	C	-0.191468	-0.152670	0.164939
17	C	-0.198968	-0.166725	0.182773
18	C	-0.152766	-0.148993	-0.108470
19	H	0.163873	0.191103	-0.007175
20	C	-0.156567	-0.151713	-0.119229
21	H	0.157103	0.185786	-0.008066
22	C	-0.145813	-0.111740	0.236586
23	H	0.156785	0.179319	0.003809
24	H	0.158032	0.180600	0.004267
25	H	0.156220	0.186280	-0.010443
26	C	0.240430	0.210606	-0.042203
27	N	-0.497438	-0.522366	0.083173
28	N	-0.072760	-0.063648	0.505598
29	N	-0.365725	-0.393925	-0.068022

Table S4. The bond orders and bond bond lengths of **1** in ground state and triplet diradical state.

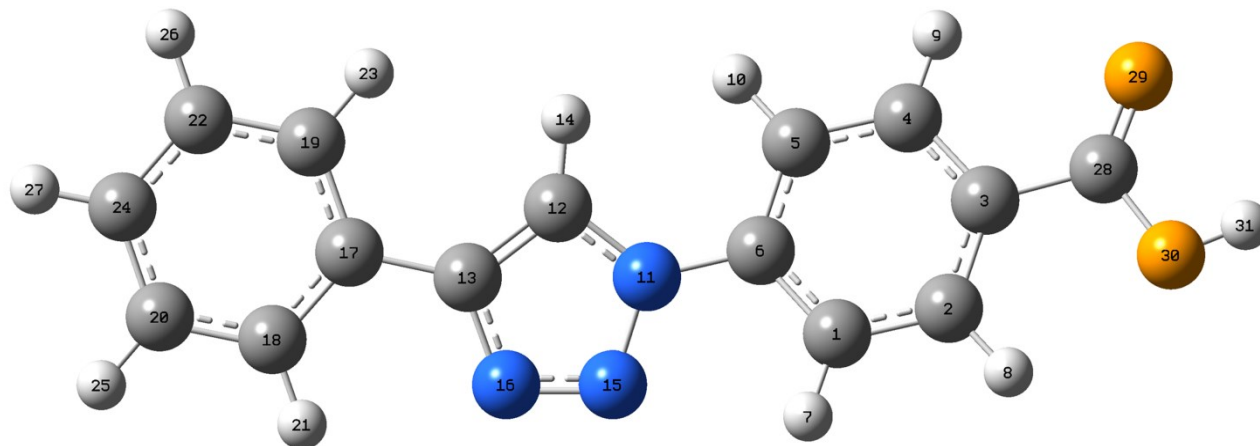
closed-shell singlet state		triplet diradical		
	bond orders		bond lengths	
	closed-shell singlet state	triplet diradical	closed-shell singlet state	triplet diradical
1(N)-2(N)	1.47779444	1.48348176↑	1.28038	1.27657↓
2(N)-3(N)	1.03959101	0.95248811↓	1.34154	1.37315↑
3(N)-17(C)	1.24665534	1.20822723↓	1.35487	1.36455↑
17(C)-26(C)	1.59254065	1.57563139↓	1.37027	1.37080↑
3(N)-4(C)	0.96899387	1.18577272↑	1.41292	1.35994↓
4(C)-6(C)	1.42181775	1.05608420↓	1.39108	1.46099↑
6(C)-7(H)	0.90401786	0.90938187↑	1.07993	1.07924↓
6(C)-8(C)	1.48592860	1.84303570↑	1.38105	1.33900↓
10(C)-19(C)	1.36384607	1.35950567↓	1.39381	1.39514↑
10(C)-26(C)	1.03970708	1.06966244↑	1.46488	1.46016↓
11(C)-24(C)	1.45950057	1.46337344↑	1.38593	1.38535↓
5(N)-27(C)	3.01910052	2.86402114↓	1.14742	1.15976↑
23(C)-27(C)	0.97140524	1.11510092↑	1.43492	1.39286↓

Table S5. Mulliken charges of **2** in ground state and Mulliken charges and spin densities of **2** in the triplet diradical state.



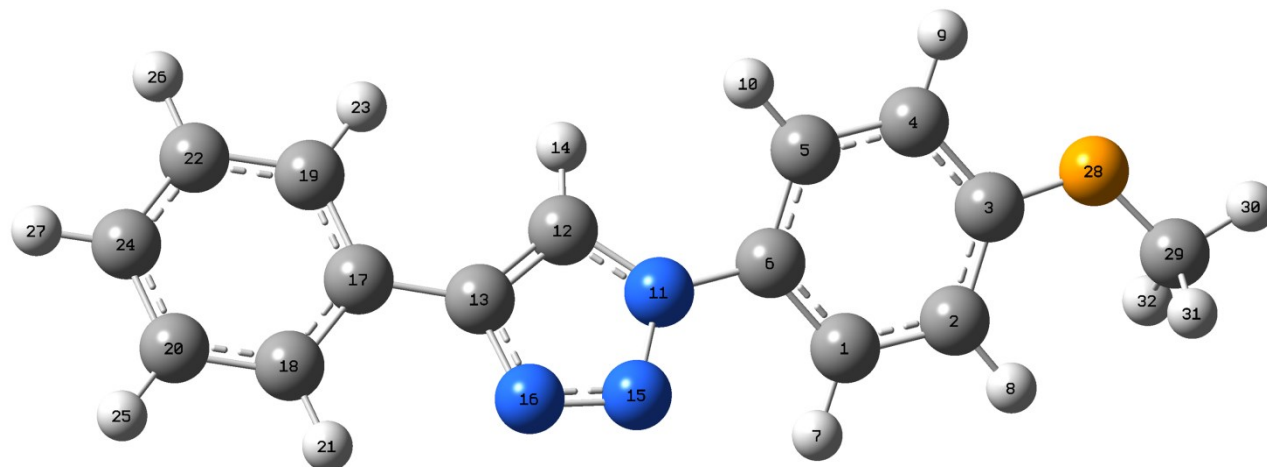
No.	Elements	Ground state	Triplet diradical	
		Mulliken charges	Mulliken charges	Spin population
1	C	-0.165188	-0.166425	0.186881
2	C	-0.176066	-0.200185	-0.065820
3	C	0.050831	0.048477	0.419286
4	C	-0.175325	-0.196616	-0.027389
5	C	-0.179302	-0.180150	0.142580
6	C	0.342424	0.299371	0.306274
7	H	0.193264	0.183384	-0.009573
8	H	0.189121	0.170880	0.000731
9	H	0.185921	0.168182	-0.000870
10	H	0.188492	0.175735	-0.007625
11	N	-0.386728	-0.349776	0.073150
12	C	0.007111	-0.012142	0.122283
13	C	0.170011	0.221274	0.195978
14	H	0.232635	0.232656	-0.006754
15	N	-0.074399	-0.071281	0.275284
16	N	-0.367455	-0.370397	0.081943
17	C	0.115763	0.110538	-0.032094
18	C	-0.192044	-0.165796	0.109625
19	C	-0.199426	-0.174413	0.109940
20	C	-0.152837	-0.149889	-0.074572
21	H	0.163481	0.184458	-0.004924
22	C	-0.156690	-0.152892	-0.072023
23	H	0.156873	0.178135	-0.004834
24	C	-0.146299	-0.121246	0.151395
25	H	0.156554	0.173406	0.002682
26	H	0.157828	0.174918	0.002569
27	H	0.156025	0.178548	-0.006677
28	C	0.613990	0.575449	0.015764
29	O	-0.514058	-0.540476	0.092511
30	O	-0.413075	-0.422457	0.022311
31	N	-0.493789	-0.500714	0.001376
32	H	0.357831	0.351086	0.001144
33	H	0.354525	0.348358	-0.000550

Table S6. Mulliken charges of **3** in ground state and Mulliken charges and spin densities of **3** in the triplet diradical state.



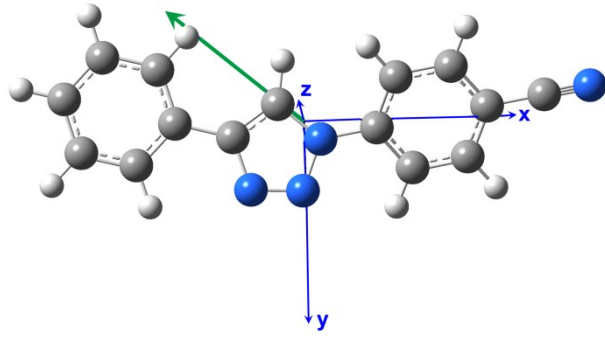
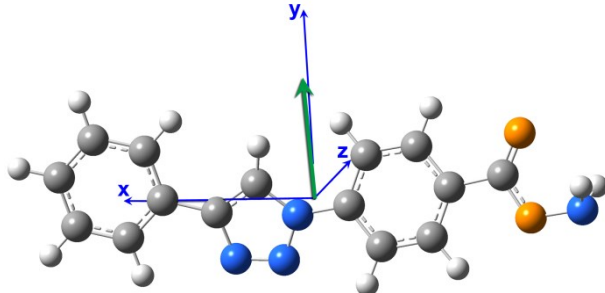
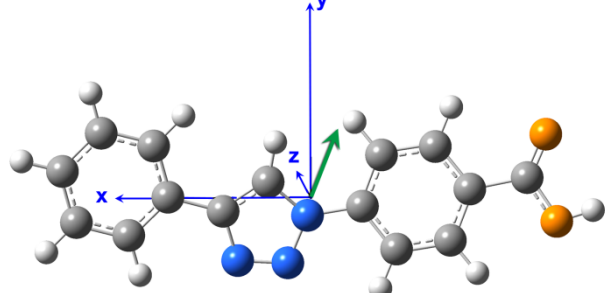
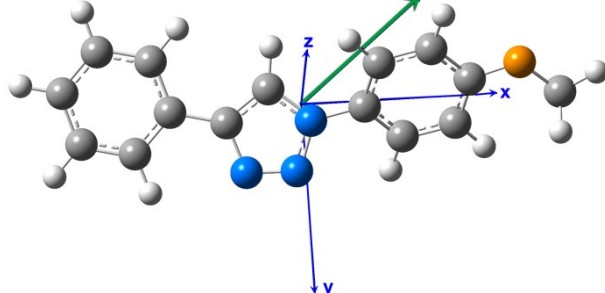
No.	Elements	Ground state	Triplet diradical	
		Mulliken charges	Mulliken charges	Spin population
1	C	-0.163899	-0.190114	0.118738
2	C	-0.179345	-0.191090	-0.063916
3	C	0.066073	0.046487	0.170297
4	C	-0.179158	-0.189266	-0.067187
5	C	-0.177939	-0.202279	0.120226
6	C	0.338941	0.321777	0.009841
7	H	0.191913	0.170145	-0.006160
8	H	0.187616	0.168130	0.002167
9	H	0.184138	0.164686	0.002306
10	H	0.187400	0.164131	-0.005640
11	N	-0.384839	-0.402548	0.075019
12	C	0.006913	0.007600	0.602514
13	C	0.169875	0.232407	0.290620
14	H	0.232283	0.230585	-0.027827
15	N	-0.075129	-0.065450	0.516517
16	N	-0.368051	-0.396820	-0.073338
17	C	0.115523	0.109166	-0.046971
18	C	-0.191913	-0.153712	0.164235
19	C	-0.199387	-0.167938	0.182772
20	C	-0.152821	-0.149482	-0.107682
21	H	0.163327	0.189806	-0.007135
22	C	-0.156653	-0.152074	-0.118842
23	H	0.156777	0.184720	-0.008065
24	C	-0.146209	-0.113131	0.232810
25	H	0.156403	0.178172	0.003792
26	H	0.157681	0.179499	0.004269
27	H	0.155872	0.184981	-0.010297
28	C	0.549042	0.524479	0.003734
29	O	-0.495866	-0.517706	0.038380
30	O	-0.590513	-0.598426	0.005439
31	H	0.441944	0.433266	-0.000616

Table S7. Mulliken charges of **4** in ground state and Mulliken charges and spin densities of **4** in the triplet diradical state.



No	Elements	Ground state	Triplet diradical	
		Mulliken charges	Mulliken charges	Spin population
1	C	-0.164799	-0.165302	0.009566
2	C	-0.220157	-0.220015	-0.006322
3	C	0.378287	0.378221	0.009446
4	C	-0.202627	-0.202217	-0.005518
5	C	-0.172301	-0.172071	0.010597
6	C	0.301356	0.301769	-0.005719
7	H	0.181724	0.182157	-0.000255
8	H	0.174924	0.175201	0.000225
9	H	0.167515	0.167799	0.000238
10	H	0.178934	0.178991	-0.000380
11	N	-0.366996	-0.370133	-0.008091
12	C	-0.001175	-0.003434	0.338570
13	C	0.168649	0.168604	-0.077769
14	H	0.225293	0.224697	-0.014969
15	N	-0.088753	-0.071196	-0.002685
16	N	-0.377509	-0.377267	0.125082
17	C	0.115523	0.101881	0.625552
18	C	-0.193297	-0.183594	0.213429
19	C	-0.200791	-0.196331	0.333346
20	C	-0.152956	-0.160229	-0.052907
21	H	0.161536	0.160459	-0.012380
22	C	-0.156853	-0.155589	-0.155896
23	H	0.155227	0.153862	-0.017783
24	C	-0.147502	-0.150035	0.726297
25	H	0.155169	0.152931	-0.001188
26	H	0.156460	0.155684	0.003470
27	H	0.154683	0.154208	-0.035665
28	O	-0.519293	-0.519010	0.001606
29	C	-0.235466	-0.235587	-0.000177
30	H	0.185335	0.185451	-0.000007
31	H	0.169993	0.170105	0.000159
32	H	0.169867	0.169989	0.000129

Table S8. Dipole moments and Cartesian coordinates for optimized molecular structures of 1–4. The green arrows denote the dipole directions.

Compounds	Dipole moment	
	Direction	Value
1		4.13 Debye
2		3.36 Debye
3		2.14 Debye
4		4.19 Debye

Cartesian coordinates of the optimized molecular structure of 1:

	X	Y	Z
C	2.27687848	-1.06714532	-0.33407757
C	3.64265883	-1.29600537	-0.29490746
C	4.51421863	-0.25554732	0.02873870
C	4.01142622	1.01653899	0.31389591
C	2.64713181	1.24614309	0.28906270
C	1.78493641	0.20009520	-0.03400995
H	1.60410712	-1.86523499	-0.61922053

H	4.03915576	-2.27616820	-0.52641635
H	4.69415245	1.81908066	0.56157537
H	2.23517077	2.22138216	0.50806647
N	0.39040609	0.44199576	-0.05899301
C	-0.63879001	-0.43668221	0.05586774
C	-1.76590717	0.34210506	-0.04292960
H	-0.48915402	-1.48814706	0.22382736
C	-3.18517686	-0.02624562	0.01003901
C	-4.16261579	0.96604830	-0.09123311
C	-3.57801199	-1.35787807	0.15747630
C	-5.50818635	0.62703484	-0.04633106
H	-3.85158743	1.99674625	-0.20640947
C	-4.92407285	-1.69309489	0.20307374
H	-2.83093741	-2.14012914	0.23671016
C	-5.89402663	-0.70110582	0.10074313
H	-6.25898033	1.40385974	-0.12841418
H	-5.21683805	-2.72973021	0.31792160
H	-6.94478013	-0.96264363	0.13495238
C	5.92954723	-0.49370396	0.06308664
N	7.06264140	-0.68675234	0.09027524
N	-0.07767378	1.69289247	-0.21787040
N	-1.35828351	1.63724168	-0.20963519

Cartesian coordinates of the optimized molecular structure of 2:

	X	Y	Z
C	-1.76207644	-1.28724638	-0.16369421
C	-3.12809996	-1.05904001	-0.18752122
C	-3.62657238	0.22662928	0.02387080
C	-2.75394096	1.28267075	0.27325179
C	-1.38718276	1.06181807	0.31319231
C	-0.89852273	-0.22255138	0.08567632
H	-1.34966905	-2.27302564	-0.32775783
H	-3.81332063	-1.87442065	-0.37826290
H	-3.16421457	2.27018732	0.44478910
H	-0.71100454	1.87548095	0.54100678
N	0.49840893	-0.46034984	0.10887847
C	1.52194583	0.41630503	-0.05604971
C	2.65386111	-0.35226448	0.06551807
H	1.36592279	1.45784814	-0.27246745
N	0.97395683	-1.70048502	0.31720979
N	2.25481443	-1.64055391	0.29233011
C	4.07045431	0.01999911	-0.02090089
C	5.05122131	-0.97338120	0.01361216
C	4.45792219	1.35662766	-0.13393126
C	6.39438504	-0.63128209	-0.06563168
H	4.74421354	-2.00775127	0.10464064
C	5.80160307	1.69500325	-0.21500837
H	3.70838498	2.14031377	-0.15151594
C	6.77473035	0.70164548	-0.18111855
H	7.14757726	-1.40958060	-0.03651699
H	6.09005050	2.73570764	-0.30123138
H	7.82359611	0.96567789	-0.24234989
C	-5.08184504	0.52919218	-0.00151167
O	-5.56513022	1.61564147	0.16368940
O	-5.81994436	-0.57781252	-0.23778654
N	-7.22340635	-0.37104155	-0.27957046
H	-7.45257497	0.07096881	0.61136123
H	-7.36207926	0.36822265	-0.96937689

Cartesian coordinates of the optimized molecular structure of 3:

	X	Y	Z
C	-2.17377135	-1.30857956	-0.22859656
C	-3.54133402	-1.08893992	-0.25985480
C	-4.05281124	0.18479679	-0.01516107
C	-3.19114289	1.23921331	0.27563409
C	-1.82313772	1.02785994	0.32304167
C	-1.32197138	-0.24529335	0.06179210
H	-1.75172052	-2.28585209	-0.41741879

H	-4.21813246	-1.90337754	-0.48253087
H	-3.61207104	2.21737829	0.47303747
H	-1.15530187	1.83873113	0.58336351
N	0.07684294	-0.47335851	0.09239143
C	1.09457065	0.41191329	-0.05995743
C	2.23157413	-0.34965969	0.06150729
H	0.93083351	1.45428982	-0.26687579
N	0.55972488	-1.71141078	0.29416478
N	1.84047813	-1.64205539	0.27715545
C	3.64635699	0.03216052	-0.01372685
C	4.63425667	-0.95085022	0.07704246
C	4.02566651	1.36652901	-0.17171943
C	5.97591527	-0.60053330	0.01030425
H	4.33370578	-1.98356907	0.20162078
C	5.36800460	1.71316919	-0.23945265
H	3.27040795	2.14195442	-0.23968607
C	6.34817533	0.73024839	-0.14820458
H	6.73455955	-1.37058979	0.08430286
H	5.64962093	2.75206415	-0.36196535
H	7.39596554	1.00077491	-0.19932916
C	-5.51224975	0.47104340	-0.04832085
O	-5.99920616	1.55011445	0.15124332
O	-6.24982435	-0.61734930	-0.33075055
H	-7.17355557	-0.33461949	-0.33040817

Cartesian coordinates of the optimized molecular structure of 4:

	X	Y	Z
C	2.49867200	1.08458200	0.33549900
C	3.86307500	0.81714000	0.36413500
C	4.33455900	-0.43485200	-0.03031300
C	3.43113100	-1.40761700	-0.46762400
C	2.07776500	-1.13342200	-0.51272800
C	1.61103300	0.11330800	-0.10001700
H	2.11634200	2.04846800	0.64390200
H	4.53979600	1.58845600	0.70421400
H	3.82179800	-2.36568400	-0.78546400
H	1.38620500	-1.87720100	-0.88959900
N	0.21839200	0.39736200	-0.12712100
C	-0.82275300	-0.45007800	0.05106100
C	-1.93758200	0.34746700	-0.07331500
H	-0.68354100	-1.49323600	0.27336200
N	-0.22155100	1.64463900	-0.34545400
N	-1.50803800	1.61966700	-0.31211700
C	-3.36240200	0.00877100	0.02179000
C	-4.32501100	1.01216200	-0.11131100
C	-3.77748700	-1.30597900	0.24301600
C	-5.67519300	0.70127500	-0.02380900
H	-3.99672700	2.02951800	-0.28390300
C	-5.12831200	-1.61341700	0.33126700
H	-3.04230800	-2.09661700	0.34645000
C	-6.08270400	-0.61024100	0.19771000
H	-6.41363100	1.48711500	-0.13034900
H	-5.43667100	-2.63768700	0.50368800
H	-7.13709200	-0.84952300	0.26557700
O	5.63835800	-0.79941400	-0.03013400
C	6.58998100	0.16155800	0.38073900
H	7.56012000	-0.32192300	0.29603100
H	6.56537200	1.04411200	-0.26604300
H	6.42321000	0.46389900	1.41945700

2. References

1. H. C. Bertrand, M. Schaap, L. Baird, N. D. Georgakopoulos, A. Fowkes, C. Thiollier, H. Kachi, A. T. Dinkova-Kostova and G. Wells, *J. Med. Chem.*, 2015, **58**, 7186–7194.
2. CrysAlisPro, Agilent Technologies, *Version 1.171.37.33*, 2014.
3. Siemens. SAINT and SHELXTL. Siemens Analytical X-ray Instruments Inc., Madison, Wisconsin, USA, 1994.
4. Spek, A. L. *PLATON*, Utrecht University: Utrecht, The Netherlands, 2001.
5. Gaussian 09, Revision A.02, M. J. Frisch, G. W. Trucks, H. B. Schlegel, G. E. Scuseria, M. A. Robb, J. R. Cheeseman, G. Scalmani, V. Barone, B. Mennucci, G. A. Petersson, H. Nakatsuji, M. Caricato, X. Li, H. P. Hratchian, A. F. Izmaylov, J. Bloino, G. Zheng, J. L. Sonnenberg, M. Hada, M. Ehara, K. Toyota, R. Fukuda, J. Hasegawa, M. Ishida, T. Nakajima, Y. Honda, O. Kitao, H. Nakai, T. Vreven, J. A. Montgomery, Jr., J. E. Peralta, F. Ogliaro, M. Bearpark, J. J. Heyd, E. Brothers, K. N. Kudin, V. N. Staroverov, R. Kobayashi, J. Normand, K. Raghavachari, A. Rendell, J. C. Burant, S. S. Iyengar, J. Tomasi, M. Cossi, N. Rega, J. M. Millam, M. Klene, J. E. Knox, J. B. Cross, V. Bakken, C. Adamo, J. Jaramillo, R. Gomperts, R. E. Stratmann, O. Yazyev, A. J. Austin, R. Cammi, C. Pomelli, J. W. Ochterski, R. L. Martin, K. Morokuma, V. G. Zakrzewski, G. A. Voth, P. Salvador, J. J. Dannenberg, S. Dapprich, A. D. Daniels, Ö. Farkas, J. B. Foresman, J. V. Ortiz, J. Cioslowski, and D. J. Fox, Gaussian, Inc., Wallingford CT, 2009.
6. E. R. Johnson, S. Keinan, P. Mori-Sánchez, J. Contreras-García, A. J. Cohen and W. T. Yang, *J. Am. Chem. Soc.*, **2010**, *132*, 6498-6506.
7. T. Lu and F. W. Chen, *J. Comput. Chem.*, 2012, **33**, 580-592.
8. S. J. Clark, M. D. Segall, C. J. Pickard, P. J. Hasnip, M. I. J. Probert, K. Refson and M. C. Payne, *Z. Kristallogr. - Cryst. Mater.*, 2005, **220**, 567–570.
9. B. Hammer, L. B. Hansen and J. K. Nørskov, *Phys. Rev. B: Condens. Matter Mater. Phys.*, 1999, **59**, 7413-7421.
10. J. P. Perdew and Y. Wang, *Phys. Rev. B: Condens. Matter Mater. Phys.*, 1992, **45**, 13244-13249.
11. D. R. Hamann, M. Schlüter and C. Chiang, *Phys. Rev. Lett.*, 1979, **43**, 1494-1497.
12. J. S. Lin, A. Qteish, M. C. Payne and V. Heine, *Phys. Rev. B: Condens. Matter Mater. Phys.*, 1993, **47**, 4174-4180.
13. F. Bassani and G. P. Parravicini, *Electronic States and Optical Transitions in Solids*; Pergamon Press Ltd.: Oxford, U.K., 1975.